BUNCH LENGTHENING RECENTLY OBSERVED AT PF-AR

T. Ieiri*, T. Kasuga, Y. Minagawa, T. Obina, KEK, Tsukuba, Japan
T. Fujita, Hiroshima University, Hiroshima, Japan

Abstract

The PF-AR (Photon Factory Advanced Ring for pulse X-rays) at KEK has been renewed to upgrade the performance. In this project, new vacuum ducts were installed with shielding bellows instead of non-shielding aluminium bellows. Thus, the coupling impedance of the ring was improved due to the shields. Measuring the bunch lengthening before and after the installation, we evaluated the longitudinal impedance of the bellows in a low bunch current. When the bunch current was high enough, a longitudinal instability was observed, accompanied by higher-order coherent synchrotron oscillations. We discuss the instability and the impedance issues based on various phenomena and calculations.

INTRODUCTION

In electron storage rings, the natural bunch length is determined by the lattice parameters. As the bunch current increases, a bunch is distorted by the interaction with its environments. A change in a bunch shape would provide information on the coupling impedance. The resistive component of the impedance induces an additional energy loss. As a result, the center of a bunch is shifted with changing its profile. According to a numerical calculation [1], it was found that the bunch length did not change very much due to the resistive impedance. On the other hand, the imaginary part of the impedance changed the bunch length due to a potential-well distortion. When a purely inductive impedance is assumed, bunch lengthening is analytically derived. We can estimate the inductive impedance from the bunch lengthening.

When the bunch current increases further, a microwave or turbulent instability takes place above the threshold, which results in increasing the energy spread. The instability appeared not only with abnormal bunch lengthening, but also with curious phenomena related to nonlinearity. Sawtooth phenomena [2] in the bunch lengthening, for example, were observed in the damping ring at SLAC. The bunch length was unstable and entered into a cycle of damping followed by blow-up. In the PF-AR, hysteresis phenomena [3] were observed, *i.e.* two bunch-lengths existed depending on the directions changing the bunch current or the cavity voltage. Two bunch lengths in the hysteresis region exhibited different synchrotron sideband patterns. It was found that the hysteresis depended on the number of cells of the accelerating cavity, *i.e.*, the strength of the cavity impedance. These phenomena are closely related to the impedance or the wakes of the rings.

* Email: takao.ieiri@kek.jp

PF-AR

The PF-AR was originally constructed as a booster of the TRISTAN electron-positron collider. The beam energy was increased to 8.0 GeV to inject a bunch into the TRISTAN ring. After completion of the TRISTAN project in 1995, the PF-AR was converted into a storage ring dedicated to pulse X-ray research at a beam energy of 6.5 GeV. However, its performance as a light source was not satisfactory. In order to improve the performance, the vacuum ducts were renewed with shielding bellows. The upgrading project for changing the impedance was completed at the end of 2001 after a one-year shutdown.

The PF-AR is a storage ring of 377 m in circumference. There are four long straight sections, each with a length of approximately 20 m. Two straight lines, east and west parts, are prepared for accelerating cavities. Alternating periodic structure (APS) cavities with multi-cells [4] were installed there to increase the beam energy up to 6.5 GeV from injection energy of 2.5 GeV. The PF-AR usually runs with a single bunch operation. The main parameters at the injection energy of 2.5 GeV are listed in Table 1.

Table 1: Main parameters at injection beam energy*

RF Accelerating Frequency, f_{rf}	508.58 MHz
Number of Particles per Bunch, N_b	7.8×10^9 / mA
Synchrotron Frequency, f_s	24 – 32 kHz
Momentum Compaction, α	0.0128
Energy Spread, δ_ε	4.4×10^{-4}
Longitudinal Damping Time, τ_d	21.6 ms
Natural Bunch Length, σ_0	8.3 – 11.7 mm

*) The energy has changed to 3.0 GeV since October 2002.

MEASUREMENT

The bunch length was measured using a method based on the beam spectrum. A bunch-length monitor detecting two frequency components in the beam spectrum under the condition of $\omega_d\sigma_t < 1$, where ω_d is the detected angular frequency and σ_t is the rms bunch length in time, indicates the rms length of a bunch in real-time, even if the bunch shape changes [5].

The bunch-length measurement was performed for the old chamber before the upgrade in 1998. Figure 1 shows that the bunch length increases slowly up to a bunch current of 8 mA, and abruptly increases by 50% together with increasing the energy spread. The jump in the bunch length indicated a clear instability threshold. Though the jump did not indicate the hysteresis region observed in

1993 [3], the bunch length was bistable around the threshold [6]. There was a difference between the two stages in 1993 and in 1998, in that the number of cavity cells was 88 cells in 1993 and reduced to 66 cells in 1998. Figure 1 also shows the calculated bunch length, assuming that the inductive impedance is 1.0 Ω. The measured bunch length agrees with the calculation in a region of relatively low current. Thus, the inductive impedance at the stage in 1998 is estimated to be 1.0 ± 0.05 Ω. On the other hand, the synchrotron sidebands were observed around a carrier of 4.29 GHz using a spectrum analyzer. The frequencies were observed at $2f_s$ and near $3f_s$ just below the threshold. The spectrum was changed above the threshold, where the fundamental synchrotron sideband, f_s, was excited together with $2f_s$, $3f_s$ and so on.

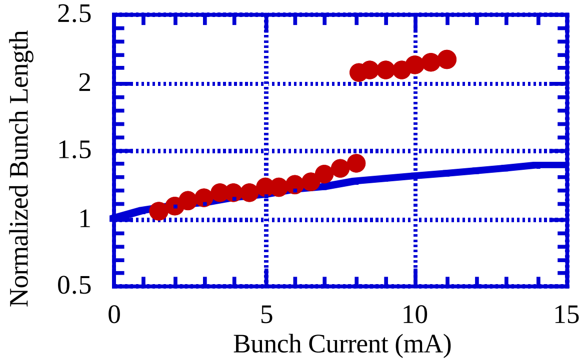

Figure 1: Bunch length normalized by the natural bunch length as a function of the bunch current for an old chamber measured in 1998 at 2.5 GeV. Dots are measured one and line is calculated bunch length based on the potential well. σ_0=12.2 mm.

A similar measurement was performed for the new chamber after the upgrade. Figure 2 shows the measured bunch length together with the calculated bunch length. The measured bunch length agrees with the calculation in a low-current region when the inductive impedance is assumed to be 0.25 ± 0.05 Ω. The measured bunch length, however, tends to deviate from the calculation above a current of 14 mA. We observed a jump in the bunch lengthening above a bunch current of 30 mA, where the specific current is much higher than that observed in the old chamber. In the high-current region, a horizontal instability was also observed, which may be discussed elsewhere [7]. On the other hand, the synchrotron sidebands were measured with the bunch current during an injection. As shown in Fig. 3, we observed a sideband frequency of 62 kHz at a current of 12 mA, which shifted to a higher frequency as the bunch current increases. The observed frequencies correspond to a synchrotron sideband of between $2.2f_s$ and $2.5f_s$. When the bunch current reached 30 mA, sidebands around fundamental synchrotron frequency were excited in addition to the higher-order synchrotron sideband.

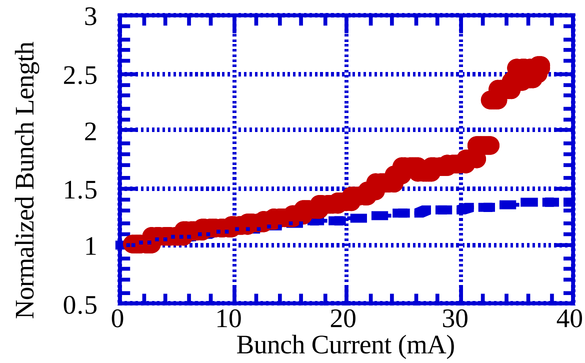

Figure 2: Normalized bunch length *vs.* bunch current for the new chamber measured in 2002 at 2.5 GeV. The dashed line is the calculated bunch length, assuming that the impedance is 0.25 Ω. σ_0=10.5 mm.

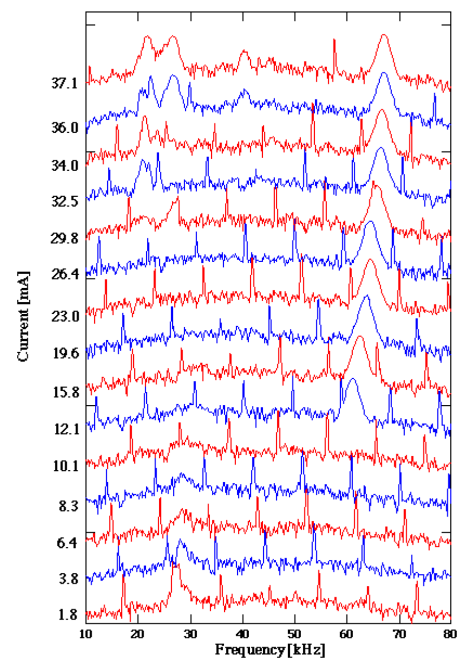

Figure 3: Sideband spectra for various bunch currents. The horizontal scale is frequency and the vertical scale is the bunch current. The spikes are the horizontal oscillation due to an injection error. f_s= 28 kHz.

DISCUSSION

Let us consider the longitudinal impedance. In the old chamber, the impedance was dominated by the APS cavities and non-shielding bellows. In the new chamber, the impedance of the bellows is negligible because of the shield; note that the cavities are the same in both stages. The wake of the cavity shows a resistive type for bunch lengths of 10 mm to 20 mm. Other dominant impedance sources are radiation masks and tapered chambers. The wakes of the masks and the tapers are inductive and contribute to bunch lengthening.

The bunch-length measurement in a low current indicates that the inductive impedance is 1.0 Ω for the old chamber and 0.25 Ω for the new one. Since the impedance of shielding bellows is negligible in the new chamber and other components, such as masks and tapers, do not much change in the upgrade, the reduction in the impedance is caused by the non-shielding bellows installed in the old chamber. Thus, the impedance of the non-shielding bellows is estimated to be 0.75 Ω from the bunch lengthening. On the other hand, the impedance of the bellows can be analytically estimated. The bellows are approximated by small cavities. Such a small cavity as illustrated in Fig. 4 behaves as inductive impedance in a region of low frequency. The impedance is given by

$$\frac{Z}{n} = -j\frac{Z_0 \omega_0 gh}{2\pi cb}, \tag{1}$$

where $n = \omega / \omega_0$ is an integer, ω_0 is the angular revolution frequency, Z_0 is the impedance of free space and c is the velocity of light. The PF-AR had about 130 bellows and each of the bellows had 12 cavities. The total impedance of the bellows is estimated to be 620 mΩ using the geometric parameters captioned in Fig. 4. The calculation is consistent with the measurement.

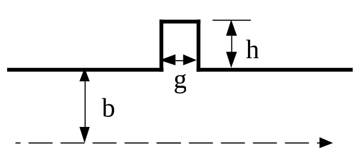

Figure 4: Sketch of a small cavity as a part of bellows, where b=40 mm, g=2 mm and h=8 mm. Note that a circular chamber is assumed instead of the actual racetrack type.

A code of the ABCI [8] calculates the wakes of the vacuum components. The masks and the tapers were modified to symmetric structures to match with the ABCI. A computer program developed by Oide [9] solves a time-dependent distribution function of a bunch using a Vlasov equation. Eigenvalues of a matrix derived from a linearized Vlasov equation were calculated using the calculated wakes. Figure 5 shows an example of the eigen-frequencies normalized by the synchrotron frequency as a function of the bunch current using the calculated wakes of the new chamber. When the bunch current reaches 10 mA, higher-order synchrotron sidebands appear with frequencies of $1.8 f_s$ and $2.6 f_s$. The frequencies change as the bunch current increases. The frequency of near f_s appears above 17 mA. On the other hand, the measurement indicated that the coherent sideband was observed between $2.2 f_s$ and $2.5 f_s$ above a current of 12 mA. Though the calculation is not precisely consistent with the measurement, excitation with higher-order synchrotron oscillation is common to both cases.

The injection energy has been lifted to 3.0 GeV from 2.5 GeV. The threshold current based on a deviation from the potential-well increased about twice, comparing Fig. 6 with Fig. 2. Considering the radiation-damping rate increases 1.73 times and the energy spread increases by 20%, the increase in the threshold current is reasonable. The deviation in the bunch lengthening from the calculation coincided with excitation of the higher-order synchrotron of $2.2 f_s$.

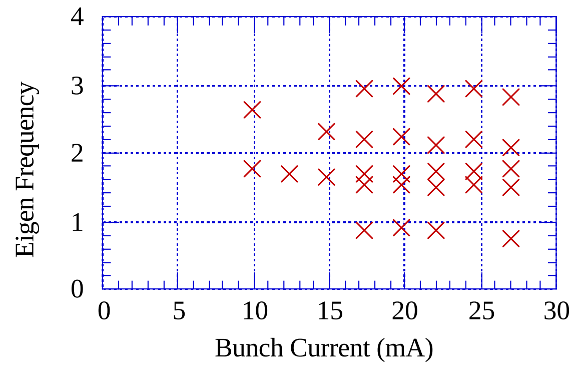

Figure 5: Imaginary part of eigenvalues normalized by synchrotron frequency as a function of the bunch current for the impedance of the new chamber. σ_0=8.75 mm. Values for Re/Damp > 0.001 are plotted.

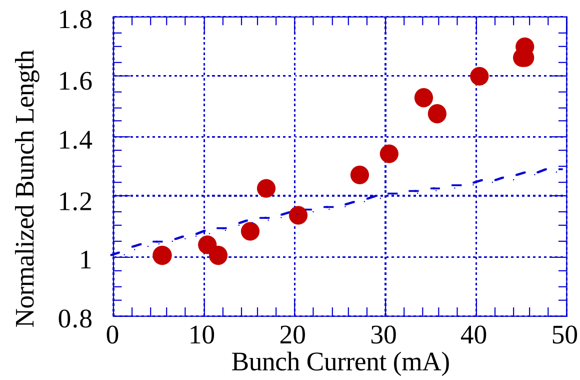

Figure 6: Normalized bunch length at a energy of 3.0 GeV. The dots are the measured bunch length; the dashed line is the calculated bunch length, assuming that the impedance is 0.25 Ω. σ_0=11.3 mm.

In summary, the relation among the impedance, the bunch lengthening and the longitudinal instability was experimentally investigated in the PF-AR. The estimated impedance of non-shielding bellows is consistent with the calculation. The longitudinal instability was observed before and after the upgrade. The jump in the bunch length shifted to a higher current due to the shielding effect of the bellows. The higher-order synchrotron signal was observed in both stages. The effect is not fully understood. Increasing the beam energy increased the instability threshold.

REFERENCES

[1] K. Bane, 1989 PAC, Chicago (1989) 789.
[2] P. Krejcik et al., 1993 PAC (1993) 3240.
[3] T. Ieiri, Nucl. Instrum. Methods A329 (1993) 371.
[4] T. Higo et al., 1984 SAST, Tsukuba, (1984) 114.
[5] T. Ieiri, EPAC 2000, Vienna (2000) 1735.
[6] T. Ieiri and T. Obina, PAC'99, NY (1999) 1135.
[7] Y. Minagawa et al., RPPB029, in these proceedings.
[8] Y. Chin, LBL-35258, UC-414 (1994).
[9] K. Oide and K. Yokoya, KEK Report 90-10 (1990).